

# Increased sensitivity through maximizing the extinction ratio of SOI delay-interferometer receiver for 10G DPSK

M. Aamer,<sup>1</sup> A. Griol,<sup>1</sup> A. Brimont,<sup>1</sup> A. M. Gutierrez,<sup>1</sup> P. Sanchis,<sup>1</sup> and A. Håkansson<sup>2,\*</sup>

<sup>1</sup>Nanophotonics Technology Center, Universitat Politècnica de València, Camino de Vera s/n, 46022, Valencia, Spain

<sup>2</sup>DAS Photonics, Camino de Vera s/n Ed 8F 2ª pta, 46022 Valencia, Spain

\*ahakansson@dasphotonics.com

**Abstract:** We present an optimized design for a 10G- differential-phase-shift-keyed (DPSK) receiver based on a silicon-on-insulator (SOI) unbalanced tunable Mach-Zehnder interferometer (MZI) switch in sequence with a Mach-Zehnder delay interferometer (MZDI). The proposed design eliminates the limitation in sensitivity of the device produced by the waveguide propagation losses in the delay line. A 2.3 dB increase in receiver sensitivity at a bit-error-rate (BER) of  $10^{-9}$  is experimentally measured over a standard implementation. The enhanced sensitivity is achieved with zero power consumption by tuning the operating wavelength or with less than 5mW for a fixed wavelength using microheaters. Also the foot-print of the device is minimized to  $0.11\text{mm}^2$  by the use of compact spirals.

©2012 Optical Society of America

**OCIS codes:** (230.3120) Integrated optics devices; (230.0230) Optical devices; (250.5300) Photonic integrated circuits.

---

## References and Links

1. A. H. Gnauck and P. J. Winzer, "Optical phase-shift-keyed transmission," *J. Lightwave Technol.* **23**(1), 115–130 (2005).
2. J. Proakis and M. Salehi, *Digital Communications*, 5th ed. (McGraw-Hill, 2008).
3. C. R. Doerr, L. Chen, B. Labs, and H. Road, "Monolithic PDM-DQPSK receiver in silicon," in *36th European Conference and Exhibition on Optical Communication* (2010), paper PD3.6.
4. C. R. Doerr, N. Fontaine, and L. Buhl, "PDM DQPSK silicon receiver with integrated monitor and minimum number of controls," *IEEE Photon. Technol. Lett.* **24**(8), 697–699 (2012).
5. K. Voigt, L. Zimmermann, G. Winzer, T. Mitze, J. Bruns, K. Petermann, B. Hüttl, and C. Schubert, "Performance of 40-Gb/s DPSK demodulator in SOI-technology," *IEEE Photon. Technol. Lett.* **20**(8), 614–616 (2008).
6. K. Suzuki, H. C. Nguyen, T. Tamanuki, F. Shinobu, Y. Saito, Y. Sakai, and T. Baba, "Slow-light-based variable symbol-rate silicon photonics DQPSK receiver," *Opt. Express* **20**(4), 4796–4804 (2012).
7. L. Zhang, J.-Y. Yang, M. Song, Y. Li, B. Zhang, R. G. Beausoleil, and A. E. Willner, "Microring-based modulation and demodulation of DPSK signal," *Opt. Express* **15**(18), 11564–11569 (2007).
8. L. Zhang, Y. Li, M. Song, R. G. Beausoleil, and A. E. Willner, "Data quality dependencies in microring-based DPSK transmitter and receiver," *Opt. Express* **16**(8), 5739–5745 (2008).
9. L. Xu, C. Li, C. Wong, and H. K. Tsang, "Optical differential-phase-shift-keying demodulation using a silicon microring resonator," *IEEE Photon. Technol. Lett.* **21**(5), 295–297 (2009).
10. S. Park, K. Yamada, R. Kou, T. Tsuchizawa, T. Watanabe, H. Fukuda, H. Nishi, H. Shinjima, and S. Itabashi, "Demodulation of 10-Gbps DPSK signals with silicon micro-ring resonators," in *23rd Annual Meeting of the IEEE Photonics Society* (2010), 264–265.
11. L. Xu, C. Li, C. Y. Wong, and H. K. Tsang, "DQPSK demodulation using integrated silicon microring resonators," *Opt. Commun.* **284**(1), 172–175 (2011).
12. Y. Ding, J. Xu, C. Peucheret, M. Pu, L. Liu, J. Seoane, H. Ou, X. Zhang, and D. Huang, "Multi-channel 40 Gbit/s NRZ-DPSK demodulation using a single silicon microring resonator," *J. Lightwave Technol.* **29**(5), 677–684 (2011).
13. L. Chen, N. Sherwood-Droz, and M. Lipson, "Compact bandwidth-tunable microring resonators," *Opt. Lett.* **32**(22), 3361–3363 (2007).

14. J. Poon, J. Scheuer, S. Mookherjea, G. Paloczi, Y. Huang, and A. Yariv, "Matrix analysis of microring coupled-resonator optical waveguides," *Opt. Express* **12**(1), 90–103 (2004).
  15. P. Dumon, W. Bogaerts, V. Wiaux, J. Wouters, S. Beckx, J. Van Campenhout, D. Taillaert, B. Luysaert, P. Bienstman, D. Van Thourhout, and R. Baets, "Low-loss SOI photonic wires and ring resonators fabricated with deep UV lithography," *IEEE Photon. Technol. Lett.* **16**(5), 1328–1330 (2004).
  16. K. Watanabe, Y. Hashizume, Y. Nasu, M. Kohtoku, M. Itoh, and Y. Inoue, "Ultralow power consumption silica-based PLC-VOA/switches," *J. Lightwave Technol.* **26**(14), 2235–2244 (2008).
- 

## 1. Introduction

Differential-phase-shift-keyed (DPSK) format exhibits several advantageous qualities [1]. It enables 3-dB improved receiver sensitivity with balanced detection, and has higher tolerance to nonlinear degradation if compared with on-off-keyed (OOK). The detection of the phase at the receiver can either be implemented using coherent or differential (non-coherent) detection. A coherent receiver uses carrier tracking by phase-locked loops to estimate the absolute phase, while in differential encoded phase-shift-keying (PSK) the information is in the phase transition and can be demodulated using a passive delay-interferometer. The simplicity of the differential detection and the elimination of a local oscillator and digital signal processor (DSP) makes differential detection advantageous for low cost links. However this comes with a loss, the differential detection has an intrinsic lower sensitivity of approximately 2dB [2].

As a technological platform, silicon-on-insulator (SOI) presents a low-cost and compact solution for mass-production of highly integrated photonic devices and has shown good potential for implementing various formats of DPSK demodulation [3–12]. The small bending radius of about 5 microns, alongside the monolithic integration of Ge photo detectors by using complementary metal-oxide-semiconductor (CMOS) compatible process makes this technology very attractive for low-cost differential receivers. Specifically in access networks at lower data speeds, such as 5Gbps or 10Gbps. Also, by implementing a polarization diversity scheme [3,4], the transversal electric (TE) and transversal magnetic (TM) polarization can be completely separated and processed individually in order to deal with problems such as polarization dependent loss and polarization dependent frequency. Rib-waveguide technology has also been proposed to achieve polarization independent performance [5], however but at expense of a larger footprint due to the higher size and bending radius of the optical waveguides.

Mainly two designs of the SOI receiver have been addressed in the literature, either using more standard Mach-Zehnder delay interferometer (MZDI) [3–6] or by using micro ring-resonators [7–12]. There are mainly two advantages of using a ring resonator in the demodulation circuit; the size and the tolerance in bit-rate deviation. However, the optimal performance is reached for an optimized Q-factor and at the same time maximized extinction ratio, which usually requires adding some tuning mechanism as in [13] and therefore increases power consumption and complexity. MZDI still seems to be the most used implementation in more complete system such as presented in [4,6].

The principle of operation of a differential demodulator using a MZDI is to superpose two adjacent bits using a delay-line (DL) so that the intensity of the superposed signal can directly be photo detected converting the differential bit-transition into an intensity variation of the signal. However, loss in the DL will result in unbalanced powers between the arms of the MZDI that will decrease the extinction ratio (ER) and hence degrade the receiver sensitivity. In this paper we demonstrate a simple approach to balance the power increasing the ER and thus enhancing the sensitivity of the DPSK receiver.

The proposed approach is based on introducing a MZI switch in cascade with the demodulation circuit in order to compensate for the propagation loss. By using this scheme a significant increase in the ER of the MZDI can be achieved from either a passive receiver, by tuning the wavelength and so achieving zero power consumption, or a low-power receiver by using a microheater. Furthermore, we also show how the footprint can drastically be reduced by using compact spirals and so minimize the size of the receiver to just a few times larger

than a ring resonator based implementation. As a proof of concept, a receiver for 10Gbps DPSK operation, where the 1-bit DL is folded into an extremely small footprint of  $0.08\text{mm}^2$ , with maximum power consumption lower than 5mW is demonstrated. Very recently, an alternative implementation based on two variable optical attenuators (VOAs) coupled to the input of each waveguide of the MZDI has also been proposed to balance the output power in a MZDI based receiver [6]. However, the overall insertion loss will suffer using this implementation since extra loss is introduced by the VOAs in the circuit. The maximum power consumption of the VOAs was also higher (17mW) than in our approach.

## 2. Design and fabrication

The schematic of the proposed DPSK demodulator is depicted in Fig. 1. A thermo-optically tunable asymmetric MZI switch is placed in series with the 10Gbps MZDI DPSK demodulator. The 10Gbps 1-bit DL is of the order of about 1cm. There are two identical inputs to the circuit and at the output of the MZDI a 2x1 multi-mode interferometer (MMI) is used. To take advantage of balanced detection this MMI should be replaced by a 2x2 MMI. Anyhow, in our test-setup we are not using balanced detection, but single detection, and hence the second output is obsolete. SOI strip waveguides with a size of  $220\times 450\text{nm}$  and surrounded by a  $\text{SiO}_2$  cladding are considered. Hence, the proposed device is optimized for TE polarization and TE gratings are used to inject/extract the light.

The asymmetric MZI switch has a length of approximately  $500\mu\text{m}$  in the shorter arm and a path difference of  $50\mu\text{m}$  between both arms. The asymmetry in the MZI introduces a wavelength switching dependency that can be used to compensate the propagation loss in the MZDI by tuning the wavelength. Alternatively, loss can also be compensated for a given wavelength by using the microheaters but at expense of consuming power. The microheaters have approximately the same length and width than the optical waveguides in the MZI arms and follow the same spiral shape shown in Fig. 1.

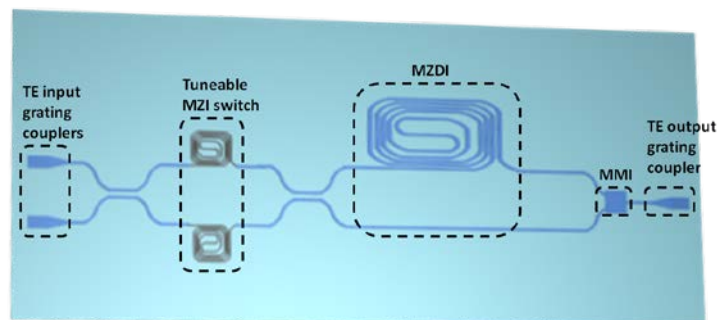


Fig. 1. Schematic of the proposed DPSK demodulator. Each square represent  $100 \times 100\mu\text{m}^2$ . From left to right in the figure: Two input TE grating couplers with waveguide tapers, 2x2 unbalanced MZI switch, MZDI with a 10GHz delay-line, a 2x1 MMI, taper, and an output grating coupler.

Figure 2 shows the simulated spectral response of the DPSK demodulator using the transfer matrix method [14]. In the simulation the 1-bit DL was set to fit a 10G symbol rate being waveguide propagation loss of 6dB/cm. Propagation loss is higher than state-of-the-art values, however it better fits the actual fabricated waveguide used here in the characterized device. DPSK demodulation can be carried out at the minimum in the transmission spectrum, given rise to an alternate-mark inversion (AMI) modulation format, or at the maximum transmittance, given rise to a duobinary (DB) modulation format. To prove the increase in performance we will here use the AMI modulation format at a minimum transmission, however DB modulation could be used in an identical manner. In both cases, the ER between minimum and maximum transmission should be maximized to enhance the sensitivity of the

receiver. To achieve this it is important that the output power in the arms of the MZDI, or in other words the amplitudes of the two adjacent bits, are identical so they completely cancel each other out maximizing the ER.

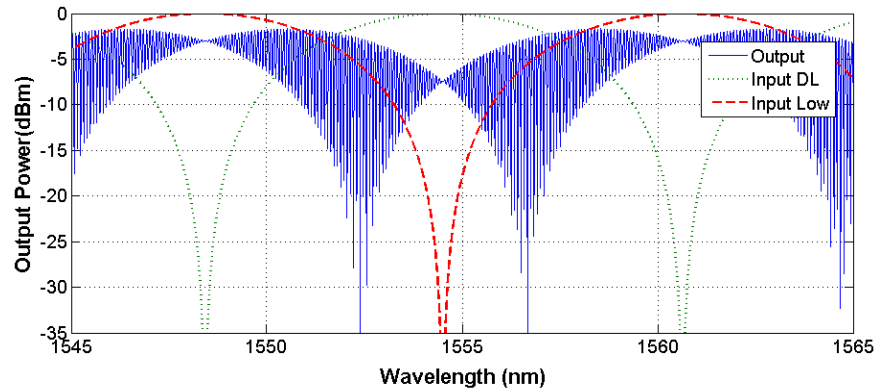


Fig. 2. Simulated spectral response at the MZDI inputs (green-dotted, red-dashed) and at the demodulator output (blue-solid).

To reflect the behavior of the MZI switch for increasing the ER, Fig. 2 includes the input power to each arm of the MZDI; the green dotted curve is the power at the input of the delay-line arm of the MZDI and the red dashed curve for the opposite arm. The two curves cross at  $-3$  dB, which corresponds to the standard 50:50 splitting ratio. It is clear from the figure that the ER at 50:50 is not the optimized value, but closer to 65:35, in order to compensate for the propagation loss in the DL. The simulation predicts an increase in ER from around 13 dB at 50:50 to more than 30 dB at maximized performance. It should be pointed out that supposing state-of-the art propagation losses [15], the theoretically maximum ER will still be limited to 16 dB for a standard 50:50 splitting ratio and therefore the proposed technique will also be required to enhance the receiver sensitivity. The impact will be lower for DPSK receivers designed for a higher bit rate because the DL will have a shorter length and thus losses will be lower. For instance, for 40 Gbps operation, the theoretically maximum ER will be around 28 dB supposing state-of-the art propagation losses. However, even in this case, a fine tuning of the splitting ratio would be useful for compensating potential undesired variations in the fabrication process that could degrade the ER.

On the other hand, the  $50\mu\text{m}$  path difference in the MZI switch results in a free spectral range (FSR)  $\sim 160$  times larger than the FSR of the MZDI, which means that between two minima of the MZI switch, there will be around 160 minima of the MZDI. Two of these set of minima would show the maximized ER, as shown in Fig. 2, and thus increased sensitivity of the receiver without requiring any active tuning on the chip. In our case, this will result in at least 5 optimized wavelength operation points, which have maximum ER, within the standard fiber optic communications C-Band, i.e. from 1530 nm to 1565 nm. For enhanced performance it is important to use a good ratio between these two FSRs. A too high ratio, i.e. a shorter path difference in the MZI switch, would not achieve the resolution between local minima needed to achieve a global optimum minimum, and a too low ratio, i.e. a longer path difference in the MZI switch, could possibly result in no optimized resonance within the operational bandwidth of the receiver.

The DPSK receiver was fabricated on SOI wafer with silicon core thickness of 220 nm and buried oxide (BOX) of  $2\mu\text{m}$ , and covered by a  $1\mu\text{m}$ -thick silica overcladding. The fabrication process was carried out by using electron beam lithography and dry etching by using inductively coupled plasma (ICP) system. Plasma enhanced chemical vapor deposition

(PECVD) was also used, to grow the overcladding silica layer. Figure 3 shows images of the fabricated MZI switch and delay-line structure.

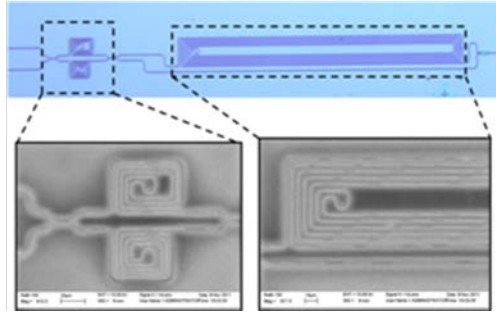


Fig. 3. Optical photo of the MZI-MZDI structure. Below the left and right inset show a SEM image of the MZI with and MZDI spirals, respectively.

### 3. Experiment and results

Continuous-wave light was generated by an external cavity laser and was first swept over the full operational wavelength bandwidth, from 1545nm to 1565nm. Figure 4(a) shows the obtained experimental spectrum for an input power of  $-4\text{dBm}$ , including zoom on the optimized performances in Fig. 4(b) around 1555.5nm. The experimental spectrum is in good agreement with the simulation result in Fig. 2. Maximized performance is achieved at approximately 65:35 splitting ratio, as predicted by simulation, resulting in 28dB ER marked as R2 in Fig. 4(b). The 50:50 splitting ratio is estimated to about 11dB. The expected 16dB resonance, if propagation losses would be reduced to state-of-the-art values, is marked with R1. To estimate the increase in the receiver sensitivity, the performance at R1 will be compared with R2.

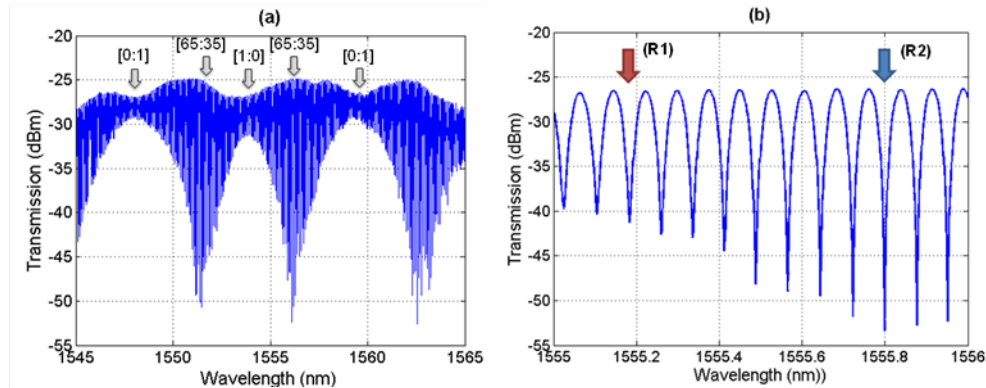


Fig. 4. Measured spectral response at the DPSK demodulator. (a) Transmission spectrum of the full experimental wavelength band. The arrows mark the different states of the MZI switch at the input of the MZDI. (b) A zoom with 1pm resolution on the wavelength range where resonances have higher ER ratio. Two resonances are marked in the figure R1 for 16dB ER and R2 with optimized 28dB ER.

As already stated, instead of varying the wavelength, by including microheaters on the MZI switch the ER of any resonance could be tuned by means of the thermo-optic effect. Figure 5 shows the ER variation for the resonance at 50:50 splitting ratio with different electrical power applied to the micro-heater on the MZI switch. Inset shows an optical photo of the metal micro heaters on-top of the MZI switch. Heaters and contact pads were sequentially patterned with lithography (PMMA resist), evaporation, and lift-off processes

and consist of 115nm thick Ti. The heater follows the same pattern as the waveguides with a width of 500 nm.

The result shown in Fig. 5 demonstrates how the ER is increased from around 11dB at 0mW to above 25 dB ER at 3mW tuning power. The efficiency could further be increased by isolating the heater and etching trenches around the structure to avoid heat dissipation [16]. If using both arms of the MZI switch, the phase can be both increased and decreased so to maximize any resonance the tuning power is equal or less than a phase shift of  $\pi$ , here corresponding to less than 5mW.

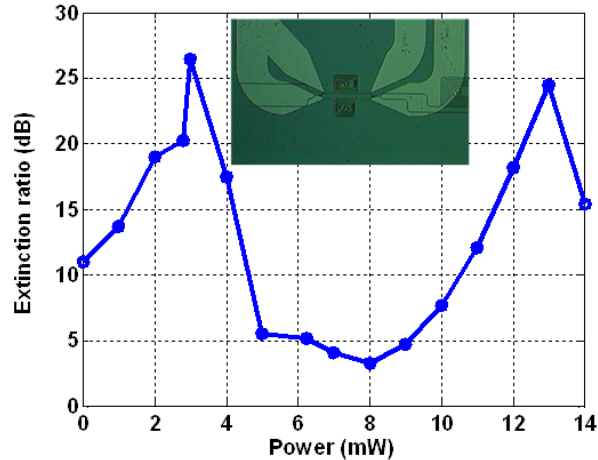


Fig. 5. ER variation for different powers applied to the micro-heater on the MZI switch. The inset shows an optical image of the microheaters on top of the MZI switch.

For system measurements and for the purpose of this study, we select the two resonances marked in Fig. 4(b); R2 with maximized performance of 28dB ER of the MZDI at 1555.80nm, and R1 with non-optimized performance of 16dB at 1555.19nm.

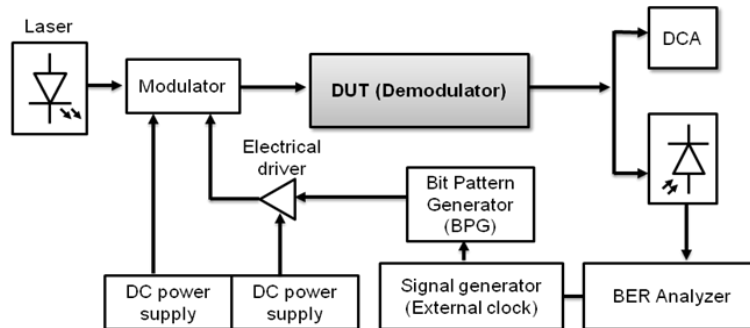


Fig. 6. Experimental set-up used for the BER measurements.

Figure 6 shows the experimental DPSK demodulation setup. To test the demodulation circuit an optical data stream was generated using a X-cut Lithium Niobate modulator biased at minimum with  $2V_{\pi}$  driving voltage. The bits was generated from a pseudorandom binary sequence pattern generator (PRBS) with a pattern length of  $2^{31}-1$  at 10-Gb/s bit-rate, delivered by a bit pattern generator (SHF BPG 44E) connected to an external clock. At the output of the chip, the demodulated signal was photo-detected by a Digital Communication Analyzer (Infinium DCA-J 86100C), and simultaneously examined on a bit error rate analyzer (SHF EA 44). The total measured insertion-loss of the chip is 21dB; 7dB loss at each grating coupler and 7dB propagation loss including about 2dB loss from the MMIs.

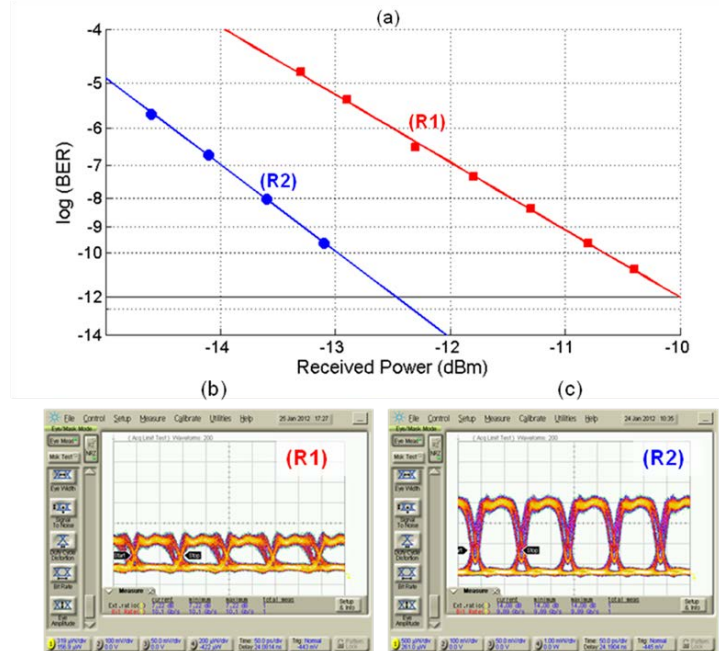


Fig. 7. System measurements at 10 Gb/s of the DPSK demodulator. (a) The graph shows the BER for the two studied resonances, R1 (red) and R2 (blue), marked in Fig. 4. (b-c) The corresponding eye diagram for R1 and R2 respectively.

Figures 7(b) and 7(c) show the eye-diagram of the two demodulated signals. It is clear that the eye is more open for the optimized resonance R2 than for R1, being the measured ER significantly improved from 7dB to 14dB. Finally, in order to estimate the increase in sensitivity of the receiver, the BER was also measured for the two resonances. Error-free operation was achieved, and the measured bit-error-rate curves are plotted in Fig. 7(a). The two curves are almost parallel and an increase in sensitivity of about 2.3dBs is measured at a BER of 10<sup>-9</sup>.

#### 4. Conclusions

We demonstrated an optimized design for DPSK receiver in SOI technology by maximizing the sensitivity with an energy efficient approach and minimizing the foot-print of the receiver. The limitation of the ER of the unbalanced MZDI produced by DL propagation losses was overcome by using an unbalanced thermo-optically tunable MZI switch in series with the MZDI. Both a passive receiver, by tuning the wavelength and so minimizing the power consumption, or a low-power receiver by using microheater (less than 5mW power consumption) were demonstrated. Two different resonances were chosen to compare optimized receiver performance with standard performance. A 2.3dB improvement in sensitivity was measured at a BER of 10<sup>-9</sup>. These results show a proof of concept how to maximize the sensitivity of low bitrates low-cost differential MZDI receivers with minimum power consumption.

#### Acknowledgments

Authors acknowledge funding by the European Commission under project HELIOS (pHotonics Electronics functional Integration on CMOS), FP7-224312. The authors would also like to thank Javier Herrera, Rakesh Sambaraju and Diedrik Vermeulen for fruitful discussion.